Statyba

ISSN: 1392-1525 (Print) (Online) Journal homepage: https://www.tandfonline.com/loi/tcem19

# A NON-LINEAR THIRD-ORDER TRIANGULAR LAMINATED PLATE ELEMENT FOR ANALYSIS OF CRACKED RC SLABS AND BEAMS

R. Belevičius , G. Kaklauskas & G. Marčiukaitis

ISSN 1392-1525. STATYBA - BUILDING CONSTRUCTION - СТРОИТЕЛЬСТВО, 1995, Nr. 2(2)



# A NON-LINEAR THIRD-ORDER TRIANGULAR LAMINATED PLATE ELEMENT FOR ANALYSIS OF CRACKED RC SLABS AND BEAMS

**R.Belevičius, G.Kaklauskas, G.Marčiukaitis**

## 1. Introduction

The use of composite materials, that is, continuous or discontinuous fibers embedded in suitable metallic or nonmetallic matrices, is receiving even wider attention and use in commercial applications. It should be noted also that almost all practical composite material structures are thin in the thickness direction because their superior properties permit the use of thin structures.

That were the reasons of exclusive activities in the field of theoretical investigations of multilayered composite plate structures. The available theoretical models for homogeneous isotropic plate structures are usually not sufficient to deal with composite where transverse shear effects can be significant even for thin multilayer composite plate structures. Considerable attention has, therefore, been given to the development of various theories of laminated composite plates. Much of this effort has been focused upon to include the effects of material orthotropy, bending-stretching coupling and transverse shear deformations. A study of Noor and Mathers [1] has shown that the inaccuracies associated with neglecting shear deformation effects in the prediction of the behaviour of laminated composite plates is a complex function of geometry, support conditions, loading, material orthotropy and laminate configuration, in addition to the thickness ratio of the plate. Therefore, reliable prediction of laminated composite plates necessitates inclusion of anisotropy, bending-stretching coupling and transverse shear flexibility in the mathematical model.

By now, about 20 shear-flexible finite element models of laminated composite plates have been proposed. Among various element shapes the triangle and quadrangle are the only desirable for practical applications. The survey of triangular and quadrilateral elements determines the Discrete Shear Triangle ( DST ) [2] as the most effective and simple composite plate element. The main limitation of DST element is, it can model only laminated plates built up with symmetric series of

layers. For a general plates with no restrictions on plies-stacking there exists only one general triangular finite element rendering satisfactory results for displacements, stresses and frequencies - element TRIPLT proposed by Lakshminarayana and Sridhara Murthy [3]. Extensive results on development of the TRIPLT for elastic composite plates \with orthotropic layers were presented by Belevicius [4].

Application of the TRIPLT element for nonlinear analysis of reinforced concrete slabs and beams was reported by Kaklauskas et al. [5]. Good match with test data was obtained for numerical examples presented.

Several approaches of nonlinear finite element analysis has been developed in recent years to model the complex behaviour of reinforced concrete (RC) slabs and beams. Four basically different approaches can be distinguished.

1) The modified stiffness approach is based on an empirical moment-curvature relationship where different flexural rigidities are assumed for different loading stages. Jofriet and McNiece [6] used a bilinear moment-curvature relation to study reinforced concrete plate bending problem. Bell and Elms [7] assumed a similar material idealisation to study slabs and shells. The models proposed by Vebo and Ghali [8] and Bashur and Darwin [9] include the non-linear variation of material properties through the depth of the slab. Finite-difference model proposed by Karpenko [10] is based on Building Code moment-curvature relationship for RC beams modified for two-way slabs with different patterns of cracking.

2) The layered model is based on the basic non-linear stress-strain law. The finite element is divided into several imaginary concrete layers each of them being considered in a plane stress state. Each layer may have different material properties corresponding to its material state. The method proposed by Hand et al. [11] for slab and shell analysis has been developed by Lin and Scordelis [12], Wanchoo and May [13], Gilbert and Warner [14], Shäfer et al. [15], Figueiras and Owen [16] and others.

3) Three-dimensional finite element modeling of RC slabs introduced by Berg et al. [17] and developed for more complex structures by Cope and Rao [18,19], etc.

4) Models based on slab analysis in which cracks are treated as lines of discontinuity of rotation angles.

This paper deals with the layered model which is based on the basic nonlinear stress-strain law. The finite element is divided into several imaginary concrete layers each of them being considered in a plane stress. Each layer may have different material properties corresponding to its material state.

## 2. Finite Element Model

The only general laminated finite element for plate bending analysis TRIPLT [3] rendering satisfactory results for displacements, stresses and frequencies has been chosen for the present work. With reference to [3], let us briefly characterise the TRIPLT element and explicitly show our way of its

formulation and derivation of all necessary matrices. The element is a shear-flexible triangular element for laminated plates taking into account the in-plane/out-of-plane couplings. It has a satisfactory rate of convergence and acceptable accuracy with mesh refinement for thick as well as thin plates of both homogeneous isotropic and laminated anisotropic materials.

The mathematical formulation is based on the Yang, Norris and Stavsky theory. Complete cubic polynomials are used to approximate the three displacements and two rotations within the element. The displacements and rotations, along with their first derivatives, are chosen as the nodal parameters. Using a local area-coordinates, explicit shape functions have been derived. All structural matrices for the element have been formulated fully analytically [4].

### 2.1. Interpolation functions

The element has three corner nodes of 15 d.o.f. per node and one centre node of five d.o.f. Complete cubic polynomials are used to approximate the three translational displacements ($v_1, v_2, v_3 = w$) and two rotations ($\theta_1, \theta_2$) within the element. The nodal parameters, 50 in all, are shown in Fig. 1, where parameters of geometry are also shown.

Denoting the cubic interpolation polynomial in area-coordinates by $\mathbf{H}$ and a vector of ten nodal parameters related to an ordinary displacement by $\{\psi\}$, after standard finite element procedure [20] we obtain the interpolation functions for displacement $v_1$ :

$$v_1 = \mathbf{H}^{\mathrm{T}}\mathbf{F}^{-1}\{\psi_{v1}\} \ , \tag{1}$$

where the inverse of configuration matrix $\mathbf{F}$ contains only differentiation coefficients of area-coordinates with respect to Cartesian ones:

$$\mathbf{F}^{-1} = \begin{bmatrix} 1 & 0 & 0 & 0 & 0 & 0 & 0 & 0 & 0 & 0 \\ 0 & 0 & 0 & 1 & 0 & 0 & 0 & 0 & 0 & 0 \\ 0 & 0 & 0 & 0 & 0 & 0 & 1 & 0 & 0 & 0 \\ 3 & c_3 & -b_3 & 0 & 0 & 0 & 0 & 0 & 0 & 0 \\ 0 & 0 & 0 & 3 & c_1 & -b_1 & 0 & 0 & 0 & 0 \\ 0 & 0 & 0 & 0 & 0 & 0 & 3 & c_2 & -b_2 & 0 \\ 0 & 0 & 0 & 3 & -c_3 & b_3 & 0 & 0 & 0 & 0 \\ 0 & 0 & 0 & 0 & 0 & 0 & 3 & -c_1 & b_1 & 0 \\ 3 & -c_2 & b_2 & 0 & 0 & 0 & 0 & 0 & 0 & 0 \\ -7 & c_2 - c_3 & -b_2 + b_3 & -7 & -c_1 + c_3 & b_1 - b_3 & -7 & c_1 - c_2 & -b_1 + b_2 & 27 \end{bmatrix} . \tag{2}$$

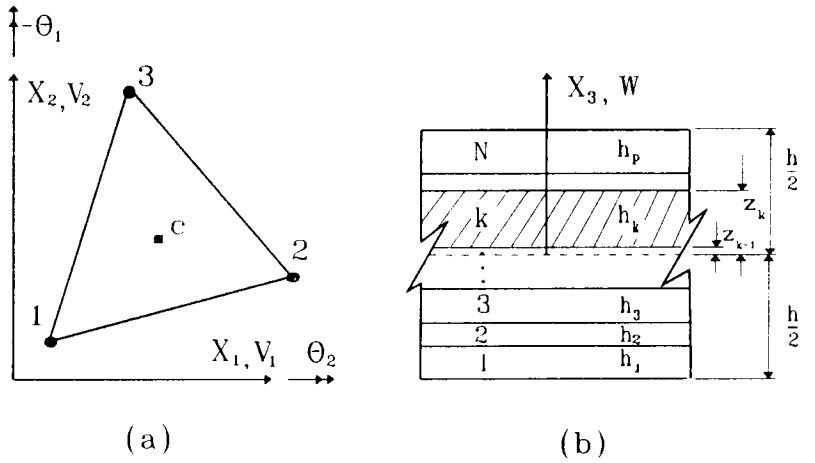


Fig. 1. Composite plate finite element TRIPLT.

( a ) Geometry, positive displacements, nodal d.o.f.:

- $v_1$, $v_{1,1}$, $v_{1,2}$, $v_2$, $v_{2,1}$, $v_{2,2}$, $w$, $w_{,1}$, $w_{,2}$, $\theta_1$, $\theta_{1,1}$, $\theta_{1,2}$, $\theta_2$, $\theta_{2,1}$, $\theta_{2,2}$ ;
- $v_1$, $v_2$, $w$, $\theta_1$, $\theta_2$ .

( b ) Composite laminate nomenclature.

Since the same finite element approximation **H** is used for the other translations and rotations we get analogously

$$
\begin{aligned}
v_2 &= \mathbf{H}^{\mathrm{T}}\mathbf{F}^{-1}\{\psi_{v2}\} \\
w &= \mathbf{H}^{\mathrm{T}}\mathbf{F}^{-1}\{\psi_{w}\} \\
\theta_1 &= \mathbf{H}^{\mathrm{T}}\mathbf{F}^{-1}\{\psi_{\theta 1}\} \\
\theta_2 &= \mathbf{H}^{\mathrm{T}}\mathbf{F}^{-1}\{\psi_{\theta 2}\}.
\end{aligned}
\tag{3}
$$

### 2.2. Behaviour of strains and stresses

Actual strains of the model are mid-surface extensional strains $\{\varepsilon^0\}$ (membrane strains), curvatures $\{\kappa\}$ and transvers shear strains $\{\gamma\}$. Assuming small strains we got those from the displacements by

$$\{\varepsilon^0\} = \begin{Bmatrix} \varepsilon^0_{11} \\ \varepsilon^0_{22} \\ 2\varepsilon^0_{12} \end{Bmatrix} = \begin{Bmatrix} v_{1,1} \\ v_{2,2} \\ v_{1,2} + v_{2,1} \end{Bmatrix} = \begin{bmatrix} \mathbf{H}^T_{,1} & \mathbf{0}^T \\ \mathbf{0}^T & \mathbf{H}^T_{,2} \\ \mathbf{H}^T_{,2} & \mathbf{H}^T_{,1} \end{bmatrix} \begin{Bmatrix} \mathbf{F}^{-1} & \{\psi_{v1}\} \\ \mathbf{F}^{-1} & \{\psi_{v2}\} \end{Bmatrix}, \tag{4}$$

$$\{\kappa\} = \begin{Bmatrix} \kappa_{11} \\ \kappa_{22} \\ 2\kappa_{12} \end{Bmatrix} = \begin{Bmatrix} -\theta_{1,1} \\ -\theta_{2,2} \\ -\theta_{1,2} - \theta_{2,1} \end{Bmatrix} = \begin{bmatrix} -\mathbf{H}^T_{,1} & \mathbf{0}^T \\ \mathbf{0}^T & -\mathbf{H}^T_{,2} \\ -\mathbf{H}^T_{,2} & -\mathbf{H}^T_{,1} \end{bmatrix} \begin{Bmatrix} \mathbf{F}^{-1} & \{\psi_{\theta 1}\} \\ \mathbf{F}^{-1} & \{\psi_{\theta 2}\} \end{Bmatrix}, \tag{5}$$

$$\{\gamma\} = \begin{Bmatrix} 2\varepsilon_{23} \\ 2\varepsilon_{13} \end{Bmatrix} = \begin{Bmatrix} w_{,2} - \theta_2 \\ w_{,1} - \theta_1 \end{Bmatrix} = \begin{bmatrix} \mathbf{H}^T_{,2} & \mathbf{0}^T & -\mathbf{H}^T \\ \mathbf{H}^T_{,1} & -\mathbf{H}^T & \mathbf{0}^T \end{bmatrix} \begin{Bmatrix} \mathbf{F}^{-1} & \{\psi_w\} \\ \mathbf{F}^{-1} & \{\psi_{\theta 1}\} \\ \mathbf{F}^{-1} & \{\psi_{\theta 2}\} \end{Bmatrix}. \tag{6}$$

Ordering the total nodal d.o.f. by

$$\{\psi\}^T = \left\{ \{\psi_{v1}\}^T, \{\psi_{v2}\}^T, \{\psi_w\}^T, \{\psi_{\theta 1}\}^T, \{\psi_{\theta 2}\}^T \right\}, \tag{7}$$

$$\{\varepsilon^0\} = \mathbf{B}^{pl}\{\psi\}, \tag{8}$$

$$\{\kappa\} = \mathbf{B}^b\{\psi\}, \tag{9}$$

$$\{\gamma\} = \mathbf{B}^s\{\psi\}. \tag{10}$$

The geometrical matrices $\mathbf{B}^{pl}$, $\mathbf{B}^b$, $\mathbf{B}^s$ are now directly readable from (4) - (10).

For a composite laminate the membrane stress resultants $\{N_{11}, N_{22}, N_{12}\}^T$, bending stress resultants $\{M_{11}, M_{22}, M_{12}\}^T$ and transverse shear resultants $\{Q_{23}, Q_{13}\}^T$ are related to corresponding strains by the following constitutive relations

$$\begin{aligned} \mathbf{N} &= \mathbf{A}\{\varepsilon^0\} + \mathbf{B}\{\kappa\}, \\ \mathbf{M} &= \mathbf{B}\{\varepsilon^0\} + \mathbf{D}\{\kappa\}, \\ \mathbf{Q} &= \bar{\mathbf{A}}\{\gamma\}. \end{aligned} \tag{11}$$

Here, using the traditional notations from laminate theory [21,22], **A, B, D** are symmetric constitutive matrices of order three and $\bar{\mathbf{A}}$ of order two. These matrices for the whole composite accumulate conventional constitutive matrices **C** of layers, assumed to be constant within the layer, i.e. from $z_{k-1}$ to $z_k$ for ply number $k$ (Fig. 1)

$$\mathbf{A} = \sum_{k=1}^{N} \mathbf{C}_k \left(z_k - z_{k-1}\right),$$

$$\mathbf{B} = \sum_{k=1}^{N} \mathbf{C}_k \frac{1}{2}\left(z_k^{\,2} - z_{k-1}^{\,2}\right),$$

$$\mathbf{D} = \sum_{k=1}^{N} \mathbf{C}_k \frac{1}{3}\left(z_k^{\,3} - z_{k-1}^{\,3}\right), \tag{12}$$

$$\overline{\mathbf{A}} = \sum_{k=1}^{N} \overline{\mathbf{C}}_k \frac{5}{4}\left(z_k - z_{k-1} - \frac{4}{3}\left(z_k^{\,3} - z_{k-1}^{\,3}\right)\frac{1}{h^2}\right),$$

where

$$\mathbf{C} = \begin{bmatrix} C_{11} & C_{12} & C_{16} \\ C_{12} & C_{22} & C_{26} \\ C_{16} & C_{26} & C_{66} \end{bmatrix}, \quad \overline{\mathbf{C}} = \begin{bmatrix} C_{44} & C_{45} \\ C_{45} & C_{55} \end{bmatrix}. \tag{13}$$

The stresses for each lamina of composite, assuming the stresses to be averaged in lamina, can be obtained from stress resultants as follows:

$$\begin{Bmatrix} \sigma_{11} \\ \sigma_{22} \\ \sigma_{12} \end{Bmatrix}_k = \mathbf{C}_k \left( \begin{Bmatrix} \varepsilon^0{}_{11} \\ \varepsilon^0{}_{22} \\ \varepsilon^0{}_{12} \end{Bmatrix} + \frac{z_{k-1} + z_k}{2} \begin{Bmatrix} \kappa_{11} \\ \kappa_{22} \\ \kappa_{12} \end{Bmatrix} \right), \tag{14}$$

$$\begin{Bmatrix} \tau_{23} \\ \tau_{13} \end{Bmatrix} = \overline{\mathbf{C}} \begin{Bmatrix} \varepsilon^0{}_{23} \\ \varepsilon^0{}_{13} \end{Bmatrix}. \tag{15}$$

The stress $\sigma_{33}$ for thin-layered composites is imperceptible in comparison with other components and is usually neglected in the analysis.

### 2.3. Finite element stiffness matrix

The $50 \times 50$ element stiffness matrix then becomes

$$\mathbf{K} = \int_{\Delta} \mathbf{B}^{pl\,\mathrm{T}} \mathbf{A}\, \mathbf{B}^{pl} d\Delta + \int_{\Delta} \mathbf{B}^{b\,\mathrm{T}} \mathbf{D}\, \mathbf{B}^{b} d\Delta + \int_{\Delta} \mathbf{B}^{pl\,\mathrm{T}} \mathbf{B}\, \mathbf{B}^{b} d\Delta$$

$$+ \int_{\Delta} \mathbf{B}^{b\,T}\,\mathbf{B}\,\mathbf{B}^{pl}\,d\Delta + \int_{\Delta} \mathbf{B}^{s\,T}\,\bar{\mathbf{A}}\,\mathbf{B}^{s}\,d\Delta\ , \tag{16}$$

where $\Delta$ is for the element area.

The five centre-node d.o.f. which are usually introduced only due to completeness requirements for the interpolating polynomials are to be eliminated. Partitioning stiffness and load matrices into two parts and denoting the parts to be eliminated by indices *2* we obtain the reduced matrices

$$\begin{aligned} \mathbf{K}_{red} &= \mathbf{K}_{11} - \mathbf{K}_{12}\mathbf{K}_{22}^{-1}\mathbf{K}_{12}^{T}\ , \\ \mathbf{P}_{red} &= \mathbf{P}_{1} - \mathbf{K}_{12}\mathbf{K}_{22}^{-1}\mathbf{P}_{2}\ . \end{aligned} \tag{17}$$

### 2.4. Basic matrices

The expressions for stiffness matrix seem to be clearly too cumbersome the conventional numerical integration or computer algebra methods to be applied directly. More oblique ways are necessary for numerical evaluation of matrices. One such way out of the situation could be the approach of *basic matrices*. The constitutive parameters (13) are assumed to be constant within each element, and thus, taking equation (16) as a whole, we see that the element geometry and the displacement assumption are described by six basic matrices of order ten defined by

$$\begin{aligned} \mathbf{T}_{ij} &= \mathbf{F}^{-T} \int_{\Delta} \mathbf{H}_{,i}\,\mathbf{H}_{,j}^{T}\,d\Delta\ \mathbf{F}^{-1}\ , \\ & \qquad ij = 00,\ 01,\ 02,\ 11,\ 12,\ 22\ , \end{aligned} \tag{18}$$

where the zero index means no differentiation. The total element stiffness matrix of order 50 separates itself into 15 ($13 \neq 0$) sub matrices of order ten according to the ordering

$$\begin{bmatrix} \mathbf{K}_{11} & \mathbf{K}_{12} & \mathbf{0} & \mathbf{K}_{14} & \mathbf{K}_{15} \\ & \mathbf{K}_{22} & \mathbf{0} & \mathbf{K}_{24} & \mathbf{K}_{25} \\ & & \mathbf{K}_{33} & \mathbf{K}_{34} & \mathbf{K}_{35} \\ & & & \mathbf{K}_{44} & \mathbf{K}_{45} \\ \textit{symm.} & & & & \mathbf{K}_{55} \end{bmatrix} \begin{Bmatrix} \{\psi_{v1}\} \\ \{\psi_{v2}\} \\ \{\psi_{w}\} \\ \{\psi_{\theta 1}\} \\ \{\psi_{\theta 2}\} \end{Bmatrix} = \begin{Bmatrix} \mathbf{P}_{v1} \\ \mathbf{P}_{v2} \\ \mathbf{P}_{w} \\ \mathbf{P}_{\theta 1} \\ \mathbf{P}_{\theta 2} \end{Bmatrix}\ . \tag{19}$$

Note that there is no coupling between in-plane translations and the out-of-plane translation.

The material parameters will be the factors in the linear combinations which give the stiffness sub matrices (19) by the basic matrices (18). The evaluation is not complicated and thus after numerous algebra we shall directly list the results

$$\mathbf{K}_{11} = A_{11}\mathbf{T}_{11} + A_{16}\left(\mathbf{T}_{12} + \mathbf{T}_{12}^{T}\right) + A_{66}\mathbf{T}_{22}$$

$$\mathbf{K}_{12} = A_{12}\mathbf{T}_{12} + A_{16}\mathbf{T}_{11} + A_{26}\mathbf{T}_{22} + A_{66}\mathbf{T}_{12}^{T}$$

$$\mathbf{K}_{14} = -B_{11}\mathbf{T}_{11} - B_{16}\left(\mathbf{T}_{12} + \mathbf{T}_{12}^{T}\right) - B_{66}\mathbf{T}_{22}$$

$$\mathbf{K}_{15} = -B_{12}\mathbf{T}_{12} - B_{16}\mathbf{T}_{11} - B_{26}\mathbf{T}_{22} - B_{66}\mathbf{T}_{12}^{T}$$

$$\mathbf{K}_{22} = A_{22}\mathbf{T}_{22} + A_{26}\left(\mathbf{T}_{12} + \mathbf{T}_{12}^{T}\right) + A_{66}\mathbf{T}_{11}$$

$$\mathbf{K}_{24} = -B_{12}\mathbf{T}_{12}^{T} - B_{16}\mathbf{T}_{11} - B_{26}\mathbf{T}_{12} - B_{66}\mathbf{T}_{12}$$

$$\mathbf{K}_{25} = -B_{22}\mathbf{T}_{22} - B_{26}\left(\mathbf{T}_{12} + \mathbf{T}_{12}^{T}\right) - B_{66}\mathbf{T}_{11}$$

$$\mathbf{K}_{33} = A_{44}\mathbf{T}_{22} + A_{45}\left(\mathbf{T}_{12} + \mathbf{T}_{12}^{T}\right) + A_{55}\mathbf{T}_{11}$$

$$\mathbf{K}_{34} = -A_{45}\mathbf{T}_{02}^{T} - A_{55}\mathbf{T}_{01}^{T}$$

$$\mathbf{K}_{35} = -A_{44}\mathbf{T}_{02}^{T} - A_{45}\mathbf{T}_{01}^{T}$$

$$\mathbf{K}_{44} = D_{11}\mathbf{T}_{11} + D_{16}\left(\mathbf{T}_{12} + \mathbf{T}_{12}^{T}\right) + D_{66}\mathbf{T}_{22} + A_{55}\mathbf{T}_{00}$$

$$\mathbf{K}_{45} = D_{12}\mathbf{T}_{12} + D_{16}\mathbf{T}_{11} + D_{26}\mathbf{T}_{22} + D_{66}\mathbf{T}_{12}^{T} + A_{45}\mathbf{T}_{00}$$

$$\mathbf{K}_{55} = D_{22}\mathbf{T}_{22} + D_{26}\left(\mathbf{T}_{12} + \mathbf{T}_{12}^{T}\right) + D_{66}\mathbf{T}_{11} + A_{44}\mathbf{T}_{00}\,. \qquad (20)$$

Now, we have separated in the stiffness matrix only six unique sub matrices **T** dependent exclusively on interpolation law. With the exclusion of the "geometry influence" the expressions of matrices to be obtained become crucially more simple. If there, no doubt, it is impossible to obtain analytical expressions neither for stiffness matrix nor for a stiffness sub matrices according to a single d.o.f., the basic matrices were obtained analytically.

### 2.5. Rotational transformations

The result (20) is based on the assumption that the material parameters behind **A**, $\overline{\mathbf{A}}$, **B**, **D** as well as the basic element matrices $\mathbf{T}_{ij}$ are all evaluated in the element coordinate system $y_1$, $y_2$. Let the laminae material description is given in coordinate system $x_1$, $x_2$, and angle $\alpha$ between coordinate systems is defined by reference to local, material system, positive anti-clockwise. The transformation of

material parameters can be given in a number of alternative forms. Here we chose the multiply angle approach, which is found to give the best insight [22] :

$$\left.\begin{matrix}(C_{11})_y \\ (C_{22})_y\end{matrix}\right\} = C_1 \pm C_2 \cos(2\alpha) + C_3 \cos(4\alpha)$$

$$(C_{12})_y = C_4 - C_3 \cos(4\alpha)$$
$$(C_{33})_y = C_5 - C_3 \cos(4\alpha)$$

$$\left.\begin{matrix}(C_{13})_y \\ (C_{23})_y\end{matrix}\right\} = \frac{1}{2} C_2 \sin(2\alpha) \pm C_3 \sin(4\alpha)$$

$$\left.\begin{matrix}(C_{44})_y \\ (C_{55})_y\end{matrix}\right\} = \frac{1}{2}( C_{44} + C_{55} )_x \pm \frac{1}{2} ( C_{44} - C_{55} )_x \cos(2\alpha) \pm$$

$$\pm (C_{45})_x \sin(2\alpha)$$

$$(C_{45})_y = (C_{45})_x \cos(2\alpha) - \frac{1}{2}( C_{44} - C_{55} )_x \sin(2\alpha) \qquad (21)$$

based on definitions

$$C_1 = \frac{1}{8}\left( 3( C_{11} + C_{22} ) + 2( C_{12} + 2C_{33})\right)_x =$$

$$= (C_{11})_x - C_2 - C_3$$

$$C_2 = \frac{1}{2}( C_{11} - C_{22} )_x$$

$$C_3 = \frac{1}{8}\left(( C_{11} + C_{22} ) - 2( C_{12} + 2C_{33})\right)_x$$

$$C_4 = \frac{1}{8}\left(( C_{11} + C_{22} ) + 2( 3C_{12} - 2C_{33})\right)_x$$

$$C_5 = \frac{1}{8}\left(( C_{11} + C_{22} ) - 2( C_{12} - 2C_{33})\right)_x =$$

$$= \frac{1}{2}( C_1 - C_4) . \qquad (22)$$

Obviously, with separation in the stiffness matrices evaluation, (20), the "material" influence, which is coordinate system dependent, and "geometry" influence, which is invariant, the coordinate system rotations for each layer of laminate can be performed very economically.

## 2.6. Non-linear procedures

For the nonlinear analysis, the direct iteration method using secant stiffness formulation is adopted. During the first iteration elastic properties of the materials are assumed. After the computation of nodal displacements, strains and curvatures at the reference plane, strains and stresses in concrete and reinforcement layers are assessed. Based on new values of secant stiffness moduli, a new stiffness matrix is formed and iterations are carried out until the convergence is achieved.

## 3. Material Model

The slab is divided into several layers, corresponding either to concrete or reinforcement. Each layer may have different properties but these properties are assumed to be constant over the layer thickness within the element. The constitutive model is based on smeared crack approach.

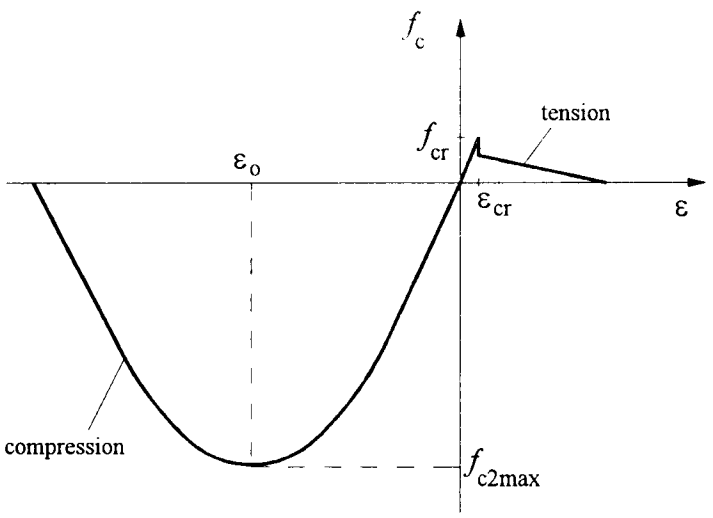


Fig. 2. Constitutive Model for Concrete

Before cracking, concrete is treated as elastic isotropic material and Poisson's ratio is assumed to be constant. Cracked concrete is considered as an orthotropic material with its first material axis normal to cracks and the second one parallel with cracks. Poisson's effect is neglected. Two models for cracked concrete have been employed:

(a) rotated crack model in which the principal axes of stresses and strains coincide,

(b) fixed crack model, in which the material axes are fixed after the crack initiation.

Perfect bond between adjacent concrete and steel layers is assumed although this is not true for advanced strain states. To model compressive concrete response, the constitutive relations offered by Vecchio and Collins in their modified compression field theory [23] have been adopted (see Fig.2). The theory estimates degradation in compressive strength due to presence of transverse tensile strain after cracking. Thus, for concrete in compression, the relation used to model work-hardening and strain softening effects is

$$f_{c2} = f_{c2\max}\left[2\frac{\varepsilon_{c2}}{\varepsilon_0} - \left(\frac{\varepsilon_{c2}}{\varepsilon_0}\right)^2\right] \tag{23}$$

where

$$f_{c2\max} = \frac{-f_c'}{0.8 - \dfrac{0.34\varepsilon_{c1}}{\varepsilon_0}} \geq -f_c'. \tag{24}$$

Here $f_{c2}$ is the average principal compressive stress in concrete; $f_{c2\max}$, the compressive strength of concrete when its degradation due to transverse tension is assessed; $f_c'$, unaxial compressive strength of concrete (cylinder test); $\varepsilon_{c1}$ and $\varepsilon_{c2}$, respectively the average tensile and compressive strain in concrete; $\varepsilon_0$, the strain in concrete cylinder at the peak stress which can be taken as $-2f_c'/E_c$ where $E_c$ is the modulus of elasticity of concrete.

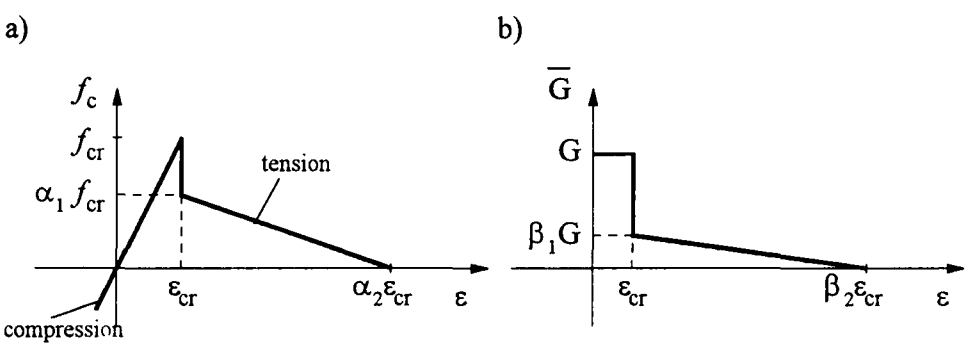


Fig. 3. Behaviour of Cracked Concrete

a - tension-stiffening diagram

b - shear retention diagram

For concrete in tension, prior to cracking a linear relation is used (Fig.3,a), i.e.

$$f_{c1} = E_c \varepsilon_{c1},\ 0 \le \varepsilon_{c1} \le \varepsilon_{cr} \tag{25}$$

where

$$\varepsilon_{cr} = \frac{f_{cr}}{E_c}. \tag{26}$$

Here $\varepsilon_{cr}$ and $f_{cr}$ are the cracking strain and stress respectively.

The cracked concrete carries between cracks a certain amount of tensile force normal to the cracked plane. The concrete adheres to the reinforced bars and contributes to overall stiffness of the structure. Several approaches [12,14,16] based on experimental results have been employed to simulate this tension-stiffening behaviour. A gradual release of the concrete stress component normal to the cracked plane is adopted in this work (Fig. 3,a).

Many experimental results have shown that for the cracked concrete the primary variable in shear transfer mechanism is the crack width, although aggregate size, reinforcement ratio, and bar size also have an influence. An approach similar to that used in ref. [24] is adopted, where the cracked shear modulus is assumed to be a function of the tensile strain (Fig. 3,b). A reduced shear modulus $\overline{G}$ is employed to simulate the aggregate interlock and dowel shear affects where $\beta_1$ is assumed to be 0.25 (Fig.3,b).

The reinforcing bars are considered as steel layers of equivalent thickness. Each steel layer exhibits an uniaxial response, having strength and stiffness characteristics in the bar direction only. A bilinear or a trilinear idealisation can be adopted in order to model the elasto-plastic stress-strain relationship.

## 4. Numerical Examples

Tension stiffening factor is considered as the most influential one in numerical modeling of cracked RC beams and slabs. In order to minimise shear effects and to eliminate some other factors, simply supported beams and one-way slabs loaded by two equal concentrated loads and, therefore, having pure moment zone have been investigated. Two such examples are presented in this paper.

### 4.1. Example 1

A simply supported beam shown in Fig. 4 was tested by Jokūbaitis [25]. The material properties and other parameters have been accepted as follows:

$f_c' = 41.3$ MPa; $f_{cr} = 3.0$ MPa; $\varepsilon_0 = -0.0021$;

$E_c = 39500$ MPa; $G_c = 15800$ MPa; $E_s = 2 \cdot 10^5$ MPa; $f_y = 587.5$ MPa;

$\alpha_1 = 1$; $\alpha_2 = 12.5$; $\beta_1 = 0.25$; $\beta_2 = 30$.

Good agreement between experimental and computed deflections (Fig.4) has been achieved at all stages of loading.

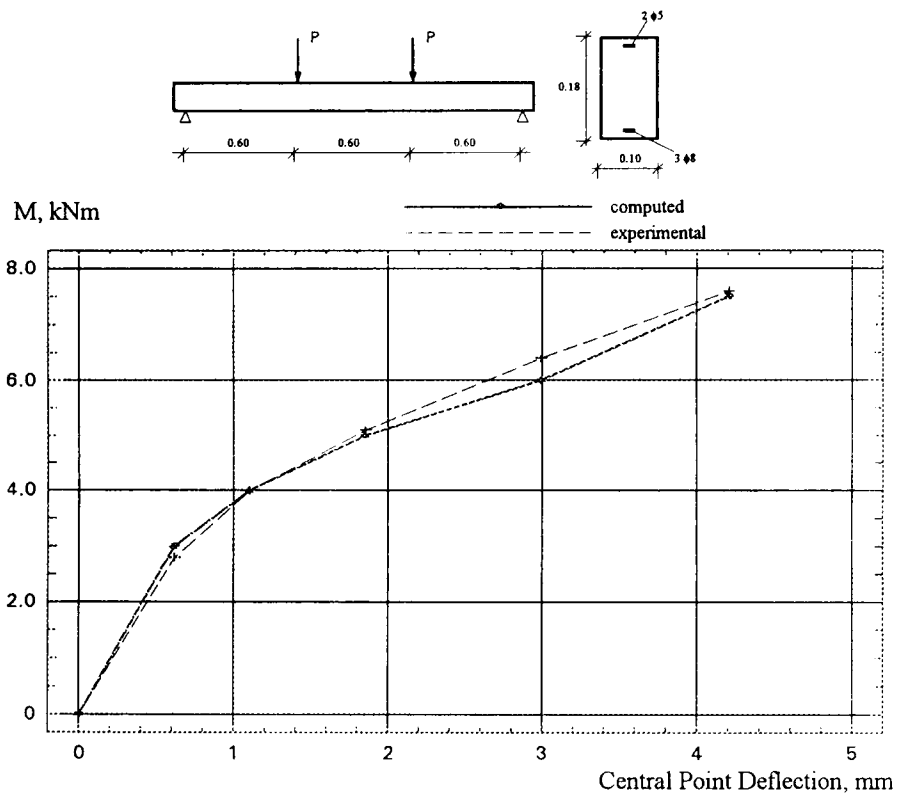


Fig. 4. Moment versus deflection curves at center point of Jokubaitis beam

### 4.2 Example 2

A simply supported one-way slab tested by Jain and Kennedy [26], was isotropically and singly reinforced with the first layer of steel in the direction of the applied uniaxial moment. A plan of the slab, indicating effective dimensions and the finite element mesh used, is shown in Fig.5. The uniaxial moment was generated by means of two uniformly distributed line loads across the slab width, symmetrically placed in respect of the centre line of the slab. The slab was 38.1 mm thick with an effective depth 31.0 mm to main reinforcement having diameter of 4.76 mm and spacing of 65.3 mm.

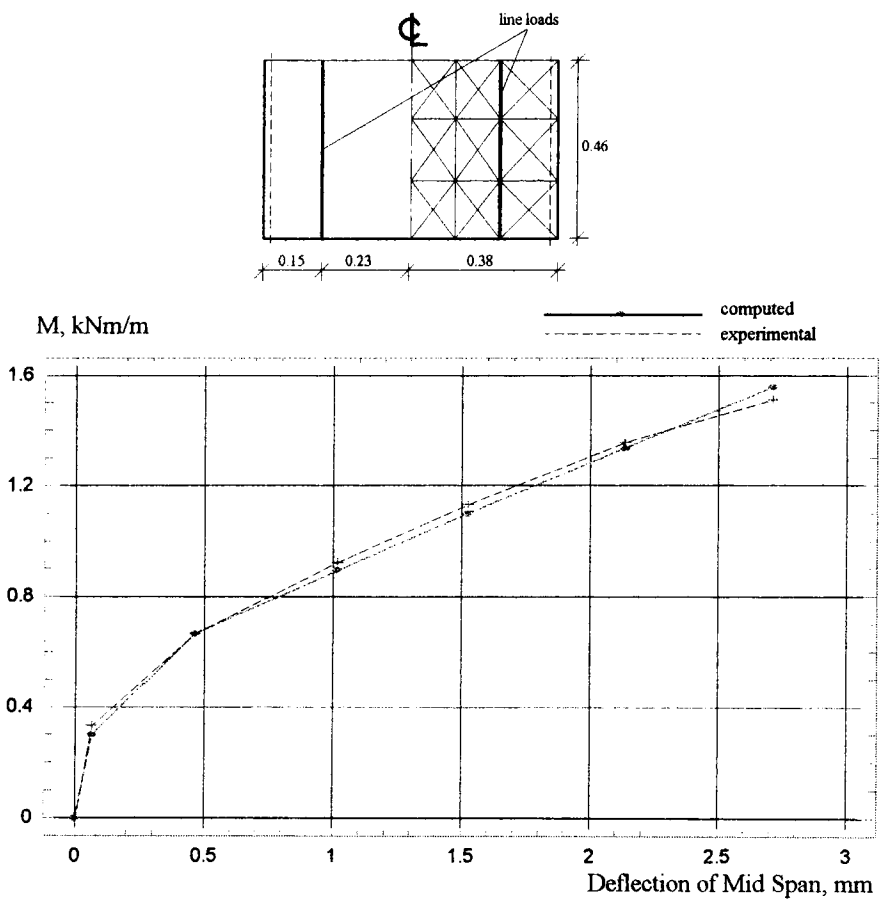


Fig.5. Moment versus deflection at midspan of Jain's simply supported one-way slab

The following material properties and parameters were assigned in the analysis:

$f_c' = 32$ MPa; $f_{cr} = 2$ MPa; $\varepsilon_0 = -0.0022$;

$E_c = 2.88 \cdot 10^4$ MPa; $G_c =$ MPa; $E_s = 2 \cdot 10^5$ MPa; $f_y = 220$ MPa;

$\nu_c = 0.18; \alpha_1 = 0.6; \alpha_2 = 12.5; \beta_1 = 0.25; \beta_2 = 30.$

The experimental and numerical moment-deflection curves are compared in Fig.5. As in the previous example, good agreement has been obtained.

## 5. Concluding Remarks

The cumbersome third-order multilayered finite element TRIPLT has been successfully applied for modeling of reinforced concrete plates and beams.

Layered approach, based on the nonlinear material model of reinforced concrete, can correctly simulate the behaviour of beams and slabs. The tension stiffening effect has a very significant influence on the post-cracking response of underreinforced concrete structures, but not on the behaviour at the ultimate load. It is believed that further interaction of numerical analyses and experiments should lead to improvement of the material model.

## Acknowledgments

The authors wish to express their sincere gratitude for the financial support received from the Lithuanian State Fund for Research and Studies.

## References

1. A.K.Noor and M.D.Mathers. Anisotropy and shear deformation in laminated composite plates // AIAA J. 14, 1976, p. 282-285.
2. P.Lardeur and J. L.Batoz. Composite plate analysis using a new Discrete Shear Triangular finite element // Int. J. Numer. Meth. in Engng. 27, 1989, p. 343-359.
3. H.V.Lakshmirayana and S.Sridhara Murthy. A Shear-Flexible Triangular Finite Element Model for Laminated Composite Plates // Int.J.Numer.Meth.Engng., 20, 1984, p. 171-187.
4. R.Belevičius. Computer Algebra in Finite Element Method. Vilnius: Technika. 1994. 154 p.
5. G.Kaklauskas, R.Belevičius, and V.Kulinič. Nonlinear Analysis of Reinforced Concrete Beams and Slabs Using Laminated Element // Proc., 4th Int. Conf. on Modern Building Materials, Structures and Techniques. Vilnius: Technika, 1995, p.177-183.
6. J.C.Jofriet and G.M.McNiece. Finite Element Analysis of Reinforced Concrete Slabs // J. Struct. Div., ASCE, 99(4), 1973, p. 853-866.

7. J.C.Bell and D.G.Elms. A Finite Element Approach to Post Elastic Slab Behavior // Special Publication SP30-15, American Concrete Institute, 1971, p. 325-344.
8. A.Vebo and A.Ghali. Moment-Curvature Relation of Reinforced Concrete Slabs // J. Struct. Div., ASCE, 103(3), 1977, p. 515-531.
9. F.K.Bashur and D.Darwin. Nonlinear Model for Reinforced Concrete Slab // J. Struct. Div., ASCE, 104(1), 1978, p. 157-170.
10. Н.И.Карпенко. Деформирование железобетона с трещинами. Москва: Стройиздат. 1976. 208 p.
11. R.F.Hand, D.A.Pecknold, and W.C.Schnobrich. Nonlinear Layered Analysis of Reinforced Concrete Plates and Shells // J. Struct. Div., ASCE, 99(7), 1973, p. 1491-1505.
12. C.S.Lin and A.C.Scordelis. Nonlinear Analysis of RC Shells of General Form // J. Struct. Div., ASCE, 101(3), 1975, p. 523-538.
13. M.K.Wanchoo and G.W.May. Cracking Analysis of Reinforced Concrete Plates // J. Struct. Div., ASCE, 101(1), 1975, p. 201-215.
14. R.I.Gilbert and R.F.Warner. Tension Stiffening in Reinforced Concrete Slabs // J. Struct. Div., ASCE, 104(12), 1978, p. 1885-1900.
15. H.Shäfer, J.Link, and G.Mehlhorn. Zur wirklichkeitsnahen Berechung von Stahlbetonplatten mit der Finite-Element-Methode // Beton- und Stahlbetonbau, 70(11), 1975, p. 265-273.
16. J.A.Figueiras and D.R.Owen. Ultimate Load Analysis of Reinforced Concrete Plates and Shells Including Geometric Nonlinear Effects. Chapter 5. Element Software for Plates and Shells, Ed. Hinton, E., Owen, D.R.J., Swansea: Pineridge Press Ltd, 1984. 327 p.
17. S.Berg, P.G.Bergan, and I.Holand. Nonlinear Finite Element Analysis of Reinforced Concrete Plates // 2nd Int. Conf. on Struct. Mech. in Reactor Tech., Berlin, Germany, Vol. M3/5. 1973.
18. R.J.Cope and P.V.Rao. Nonlinear Finite Element Analysis of Concrete Slab Structures // Proc., Inst. Civ. Engrs., Part 2, 63, 1977, p. 159-179.
19. R.J.Cope. Material Modeling of Real, Reinforced Concrete Slabs // Proc., Int. Conf. on Coputer-Aided Analysis and Design of Concrete Struct., Split, Yugoslavia, 1984, p. 85-117.
20. O.C.Zienkiewicz and R.L.Taylor. The Finite Element Method. McGraw-Hill. 1991. 648 p.
21. R.M.Jones. Mechanics of Composite Materials. Hemisphere Publishing Corporation, 1975. 520 p.
22. J.R.Vinson and R.L.Sierakowski. The Behaviour of Structures Composed of Composite Materials. Martinus Nijhoff, 1986. 450 p.
23. F.J.Vecchio and M.P.Collins. The Modified Compression Field Theory for Reinforced Concrete Elements Subjected to Shear // J.Amer.Concrete Inst., 83(2), 1986, p. 219-231.
24. L.Cedolin and S.Deipoli. Finite Element Studies of Shear-Critical RC Beams // J.Engrg.Mech.Div., ASCE, 103(3), 1977, p. 395-410.

25. V.Jokūbatis. Dėsningų ir atsitiktinių plyšių įtaka armuotų betoniniu sijų deformacijoms veikiant trumpalaikei apkrovai // Disertacija technikos mokslų kandidato laipsniui įgyti, Kauno politechnikos institutas, 1967. 235 p.
26. S.C.Jain and J.B.Kennedy. Yield Criterion for Reinforced Concrete Slabs // J.Struc.Div., ASCE, 100(3), 1974, p. 631-644.

## TREČIOS EILĖS TRIKAMPIO SLUOKSNIUOTO ELEMENTO PANAUDOJIMAS SUPLEIŠĖJUSIŲ GELŽBETONINIŲ PLOKŠČIŲ IR SIJŲ ANALIZEI

**R.Belevičius, G.Kaklauskas, G.Marčiukaitis**

Santrauka

Straipsnyje pateiktas universalus sluoksniuotos plokštės netiesinės medžiagos baigtinių elementų modelis, pritaikytas supleišėjusios gelžbetoninės plokštės skaičiavimui. Pasirinktas sudėtingas analitiškai suformuotas trečios eilės trikampis sluoksniuotas Reisnerio-Mindlino plokštės elementas, turintis 50 laisvės laipsnių. Programa įvertina atskirų plokštės sluoksnių netiesines deformacijas, supleišėjimą. Betono fizikiniame modelyje įvertinta tempiamo ir gniuždomo betono įtempimų-deformacijų diagramos žemyn krentanti dalis. Skaičiavimo modelis ir programa patikrinti, atlikus turimų ir teorinių rezultatų palyginimą. Straipsnyje pateiktų gelžbetoninės sijos ir plokštės paskaičiuoti įlinkiai gerai atitiko eksperimentinius.